



# Dependence of the physical properties of $\text{SiN}_x\text{:H}$ films deposited by the ECR plasma method on the discharge size

S. Garcia, J.M. Martin, I. Martil<sup>\*</sup>, G. Gonzalez-Diaz

*Dpto. de Electricidad y Electronica, F. Fisicas, Universidad Complutense, Madrid 28040, Spain*

Received 18 March 1997; accepted 18 June 1997

## Abstract

$\text{SiN}_x\text{:H}$  films have been deposited using two different ECR plasma sources attached to a similar deposition chamber, a Compact source and an AX4500 source both from Astex. The sources mainly differ in the discharge volume,  $55\text{ cm}^3$  and  $936\text{ cm}^3$ , respectively. Microwave power and  $\text{N}_2/\text{SiH}_4$  gases flow ratio have been varied to deposit the films. Deposition rate, infrared absorption spectra, refractive index ( $n$ ), and optical band gap ( $E_g$ ) of the films have been measured. Optical diagnosis spectra of the discharges have been recorded during the depositions. Different performances of the sources reflected in the film characteristics have been found. The properties of the films deposited using the Compact source correspond to films with compositions that range from Si-rich to near stoichiometric ones, while when using the AX4500 reactor, the film properties correspond to compositions close to the stoichiometric films or to N-rich ones. When changing from the Compact source to the AX4500 reactor, the signal corresponding to  $\text{N}_2^+$  ions and to the excited species,  $\text{N}_2^*$ , are higher in the AX 4500 than in the Compact one, the deposition rate being higher in the AX 4500 source. The different performances of the sources have been attributed to the different discharge size and diffusion length, being optimal in the case of the AX4500 source. © 1998 Elsevier Science S.A.

**Keywords:**  $\text{SiN}_x\text{:H}$  films; Electron cyclotron resonance plasma deposition; Thin film deposition

## 1. Introduction

During the last years, there has been a wide use of Electron Cyclotron Resonance (ECR) discharges for etching and thin film deposition, with results that reveal the suitability of this plasma technique for these processes [1–4]. Attending to the deposition of thin films such as  $\text{SiN}_x\text{:H}$ , excellent results attained with the ECR plasma deposition method have been published, which have improved those obtained using traditional rf plasmas, in aspects such as the hydrogen content of the films or the deposition temperature [5,6]. In spite of its wide use and of the good results attained, important questions such as the influence of different designs and sizes of the plasma sources on the film properties remain unanswered. The dependence of the performance of the plasma sources and the plasma characteristics on these aspects is known [7], and so, the influence that source characteristics (such as the discharge size) have on the properties of the deposited films should be derived from this. These questions are to be solved in order to improve all these parameters for the

deposition of optimum quality films.

In this work, we present data about the properties of  $\text{SiN}_x\text{:H}$  films deposited using two commercial ECR plasma sources of different sizes, both from Astex. We first use a Compact-ECR reactor attached to a deposition chamber of our design. After that, we substitute the Compact source by an AX4500 reactor, located on the same deposition chamber by only changing the aperture of the chamber top to accommodate the different flanges that both reactors use. The source names used correspond to those commercial ones. Characterization of the sources using the  $\text{SiN}_x\text{:H}$  film properties is made, and some results about optical diagnosis of the discharge complete the analysis of the performances of both plasma reactors.

## 2. Experimental

### 2.1. Plasma source description

The Compact-ECR source is a small size reactor designed for its application to MBE machines. The quartz liner that the reactor has inside the plasma chamber to protect the films from metal contamination of the walls has

<sup>\*</sup> Corresponding author. e-mail: imartil@eucmax.sim.ucm.es.

an inner diameter smaller than the critical size determined by the cutoff frequency of the microwave field (7.2 cm at the 2.45 GHz excitation frequency used for this study). The height ( $L$ ) and the diameter ( $2r$ ) at the output of the liner, which are the dimensions that delimit the discharge size, are 13.3 cm and 2.3 cm, respectively, which means a discharge volume ( $V = \pi r^2 \times L$ ) of 55 cm<sup>3</sup>. The AX4500 source is a reactor of moderate size which substitutes the liner by a quartz bell-jar bigger than the liner. In this case, the discharge is contained in the bell-jar, which delimits its volume. The height and the inner diameter at the output of this piece are 9.0 cm and 11.5 cm, respectively, which represents a discharge volume of 936 cm<sup>3</sup>.

Both sources are of the waveguide applicator type, with two stub-tuners to accommodate the impedance of the microwave field to the discharge. One coil around the source is used to create the ECR zone and the divergent magnetic field which extracts the excited and charged particles from the plasma source to the deposition chamber. The output of both sources, from which  $L$  is measured, is located on the top plane of the deposition chamber. The height and the inner diameter of the deposition chamber are, respectively, 25 cm and 28 cm. A gas dispersal ring of 10-cm diameter is located inside the deposition chamber 4 cm away from its top plane. The vacuum system, which consists of a turbomolecular (200 l/s) and a rotary pump, is located at the bottom of the whole deposition system. The basic design of both reactors is not changed, and only small differences in the current of the electromagnet are needed to initiate and sustain the discharge.

The comparison of the film properties obtained using both sources has been made under identical experimental conditions. N<sub>2</sub> gas, introduced on the top of the plasma source, and pure SiH<sub>4</sub>, introduced into the deposition chamber through the gas dispersal ring, are used to deposit the SiN<sub>x</sub>:H films. The substrate holder is located 14 cm away from the top plane of the deposition chamber. The deposition temperature is that determined by the plasma heating, always below 40°C. Microwave power and

N<sub>2</sub>/SiH<sub>4</sub> gases flow ratio ( $R$ ) are used as deposition parameters varied, respectively, between 50 and 200 W and 1.6 and 9. The measured reflected power is always in the 7–8 W range. The pressure is kept constant at 0.6 mTorr by always using a similar total gas flow, nitrogen plus silane, of 10.5 sccm.

## 2.2. Characterization techniques

Infrared spectra of the films, recorded with a FTIR Nicolet 5PC spectrometer in the mid infrared region (400–4000 cm<sup>-1</sup>), are used to study the bonding structure and to calculate the hydrogen content of the films [8]. This characterization is performed on films deposited on silicon substrates of high resistivity (80 Ωcm) polished by both sides. Transmittance and reflectance of the film/quartz system, measured in a Perkin-Elmer Lambda9 spectrophotometer operating in the 200–2500 nm range, are used to obtain the refractive index ( $n$ ) dispersion law and the absorption coefficient ( $\alpha$ ) of the SiN<sub>x</sub>:H films. The calculation method used allows also to know the film thickness [9]. The  $n$  values here presented are those obtained from the dispersion law at 633 nm. The optical band gap ( $E_g$ ) of the films is calculated by fitting the  $\alpha$  values to the well known Tauc plot for  $\alpha > 10^4$  cm<sup>-1</sup>. More details about the different characterization techniques used can be found elsewhere [6,10,11].

Optical diagnosis of the discharge is also used to analyze the performance of the sources. The spectra are recorded through a quartz window (with transmission close to 100% in the 100–1000 nm range) located in one side of the deposition chamber by using a monochromator (Jovin Ivon H25) operating in the 200–800 nm. The analyzed spectra correspond to the whole downstream volume, as no optical elements are employed to focus the light from the discharge. A R-446 Hamamatsu photomultiplier and a RIBER multiplier are used to convert and amplify the signal, which is recorded in a personal computer by using a data acquisition card.

Table 1

Si–H and N–H bond density ([Si–H], [N–H] respectively) and hydrogen content ([H]) for films deposited at different N<sub>2</sub>/SiH<sub>4</sub> ratios and microwave powers using both reactors

Power (W)	Compact-ECR			AX4500		
	[Si–H] ( $\times 10^{22}$ cm <sup>-3</sup> )	[N–H] ( $\times 10^{22}$ cm <sup>-3</sup> )	[H] ( $\times 10^{22}$ cm <sup>-3</sup> )	[Si–H] ( $\times 10^{22}$ cm <sup>-3</sup> )	[N–H] ( $\times 10^{22}$ cm <sup>-3</sup> )	[H] ( $\times 10^{22}$ cm <sup>-3</sup> )
100	0.55	1.33	1.88	–	2.36	2.36
100	0.98	1.02	2.00	–	1.03	1.03
100	2.03	0.68	2.71	0.29	1.17	1.46
100	2.41	0.56	2.97	0.73	0.52	1.25
200	0.39	3.83	4.22	–	1.85	1.85
150	0.81	1.91	2.72	–	1.42	1.42
100	2.03	0.68	2.71	0.29	1.17	1.46
50	2.44	0.30	2.74	0.67	1.02	1.69

### 3. Results

#### 3.1. Dependence of film properties on $N_2/SiH_4$ ratio

Fig. 1a shows the deposition rate of the films at 100 W as a function of the ratio  $R$  for both reactors. For both of them, the deposition rate increases with decreasing  $R$  (i.e., higher  $SiH_4$  flows), indicating that the formation of the film is limited by the rate of arrival of silane species to the substrate, as is usually observed in plasma deposited  $SiN_x:H$  films. From the figure, it is clear that the deposition rate is much higher for the AX4500 source than for the Compact one (by more than three times in all cases), with a more pronounced increase at the lowest  $R$  values. This would indicate that the nitrogen species are more effectively excited in the discharge generated by the AX4500 reactor to promote reactions in vapor phase between them and the silane radicals, which result in the film formation.

In the upper part of Table 1, we presents the Si–H and N–H bond density ([Si–H] and [N–H], respectively) and the hydrogen content ([H]) for films deposited at 100 W and different  $R$  values with both sources. Attending to the Si–H bond density, a significant decrease is observed for all  $R$  values when comparing the density obtained with the AX4500 to that obtained with the Compact source, meanwhile the N–H bond density is almost similar in both sources for all  $R$  values except for the highest one. As can be observed in the table, those facts result in a clear decrease of the total H content in the films using the AX4500 source, except at high  $R$  values, for those the N–H bond density is clearly higher in the AX4500 reactor. The hydrogen content of the films deposited with this source is really low if we consider that the depositions are carried out at room temperature, with the minimum value ( $1.03 \times 10^{22} \text{ cm}^{-3}$ ) corresponding to the 10 atomic percentage. The bond density related to hydrogen in both sources reveal that the films deposited with the Compact reactor at 100 W power are Si-rich, as we have already explained in previous works [6,11], and that those deposited with the AX4500 source are stoichiometric or N-rich, as the H atoms incorporated into the silicon nitride network are primary bonded to the N ones [12], except for the lowest  $R$  value. This trend supports the idea discussed above, that is, the nitrogen species in the AX4500 discharge are more effectively excited to react with the silane radicals for incorporating N atoms into the silicon network, which would result in films with characteristics close to those of the stoichiometric compound or corresponding to N-rich composition.

Fig. 1b shows the position of the Si–N vibration mode in the infrared spectra as a function of  $R$ . Attending to the results obtained using the Compact source, the films deposited at the lowest  $R$  values (1.6–3) are Si-rich, as is deduced from the lower frequencies of this peak than the corresponding one to the stoichiometric compound (830

$\text{cm}^{-1}$ ) [13]. For the other  $R$  values, the peak positions are in good agreement with the value expected for stoichiometric films. For the films deposited with the AX4500 source, it seems that the peak position corresponds to that of the stoichiometric compound in all cases, even at the lowest  $R$  values. The increase observed at the highest  $R$  value is explained by the higher N–H bond density measured in this film, as it is known that the Si–N peak position shifts to higher frequencies with the [N–H], being located at positions higher than  $850 \text{ cm}^{-1}$  for [N–H] higher than  $\sim 2.0 \times 10^{22} \text{ cm}^{-3}$  [14]. For all films deposited using this source, the positions of the Si–H vibration mode (not shown here) are in the  $2170\text{--}2190 \text{ cm}^{-1}$  range, slightly higher than that obtained for plasma deposited films (around  $2160 \text{ cm}^{-1}$ ) [4,13]. This could be

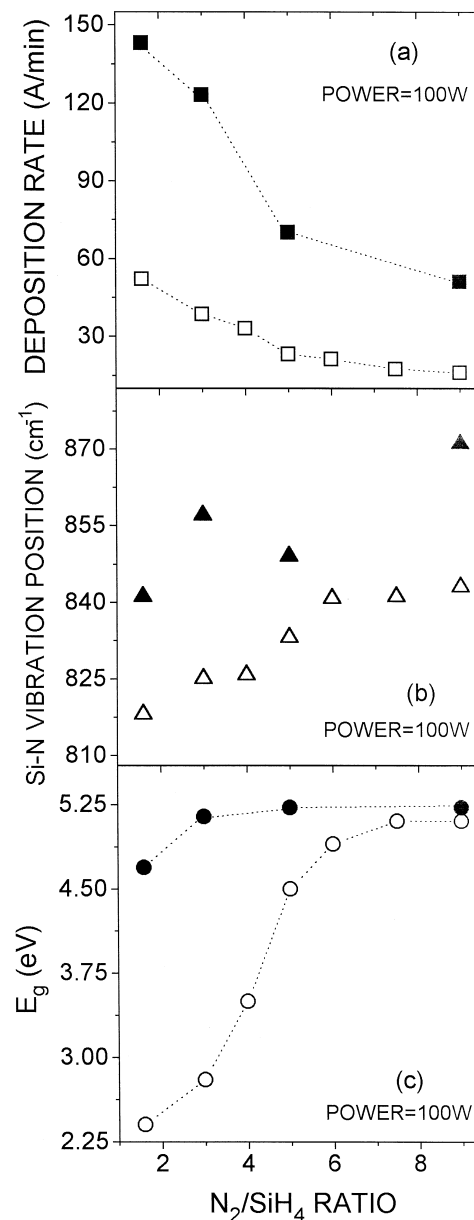


Fig. 1.

attributed to the N-rich character that these films present in general, as it is known the appearance of a component of the Si–H peak at  $2100\text{ cm}^{-1}$  which shifts this peak to higher frequencies as N atoms substitute the Si ones in the silicon nitride network [15]. The Si–H peak shifts to higher frequencies in the films deposited using the Compact source as the film character changes from Si-rich to N-rich [6].

Fig. 1c presents the  $E_g$  values calculated for the films as a function of the  $\text{N}_2/\text{SiH}_4$  ratio. The different performances discussed for both sources are clearly observed in this plot. As it is known for plasma deposited  $\text{SiN}_x\text{:H}$  films, the optical band gap increases with the N content of the film, approaching the value corresponding to the stoichiometric compound, 4.7 eV [11]. According to that, this

figure would indicate that the films deposited using the Compact source correspond to compositions comprised in a wide range, from very Si-rich to near stoichiometric ones. In the case of the films obtained with the AX4500 reactor, the  $E_g$  values of all films are at least that of the stoichiometric compound, and the increase observed above this value confirms the N-rich character of these films, in agreement with the high N–H bond density that the films contain. The  $n$  values agree with this supposition, as they vary between 2.27 and 1.80 and between 2.15 and 1.90 for the Compact and AX4500 sources, respectively, with lower values corresponding to higher  $R$ .

### 3.2. Dependence of film properties with microwave power

Fig. 2a shows the deposition rate of the films as a function of the microwave power at  $R=3$ . For both sources, the deposition rate increases with the power, with different variation rates for each of them. Thus, the deposition rate with the Compact source increases by almost 4 times when the power is changed from 50 to 200 W, meanwhile the increase observed with the AX4500 reactor is much smaller (it increases by 1.5 times when the power changes in the same values). This indicates that the activation of the discharge clearly varies with the microwave power in the Compact reactor, meanwhile it is less dependent on this deposition parameter in the AX4500 source. Attending to the values obtained at each power for both sources, the reactions between nitrogen and silane species appear to be more activated in the AX4500 source, as the deposition rate is higher than that obtained for the films deposited with the Compact reactor in all cases.

Table 1 includes the [Si–H], [N–H] and [H] values calculated for the films deposited at  $R=3$  using different power values (lower part of the table). The results presented there clearly show that the Si–H bond density is much higher in the films deposited using the Compact source than in those deposited using the AX4500. Attending to the N–H bond density, it should be noticed the wider range of values obtained for the films deposited with the Compact source compared to that calculated for the films deposited using the AX4500 reactor. Regarding to the hydrogen content, it is clearly lower in the AX4500 source, mainly due to the lower Si–H bond density. The relation [Si–H]/[N–H] indicates that the films deposited with the AX4500 source are N-rich in all cases, meanwhile those deposited with the Compact reactor have a composition that varies between Si-rich and stoichiometric or N-rich with increasing powers.

Fig. 2b presents the Si–N vibration mode position as a function of the microwave power at  $R=3$  for the two reactors used. It can be observed that it follows a similar trend to that described with respect to the variation with the  $\text{N}_2/\text{SiH}_4$  ratio, indicating again the different composition ranges of the films deposited with both reactors previously discussed.

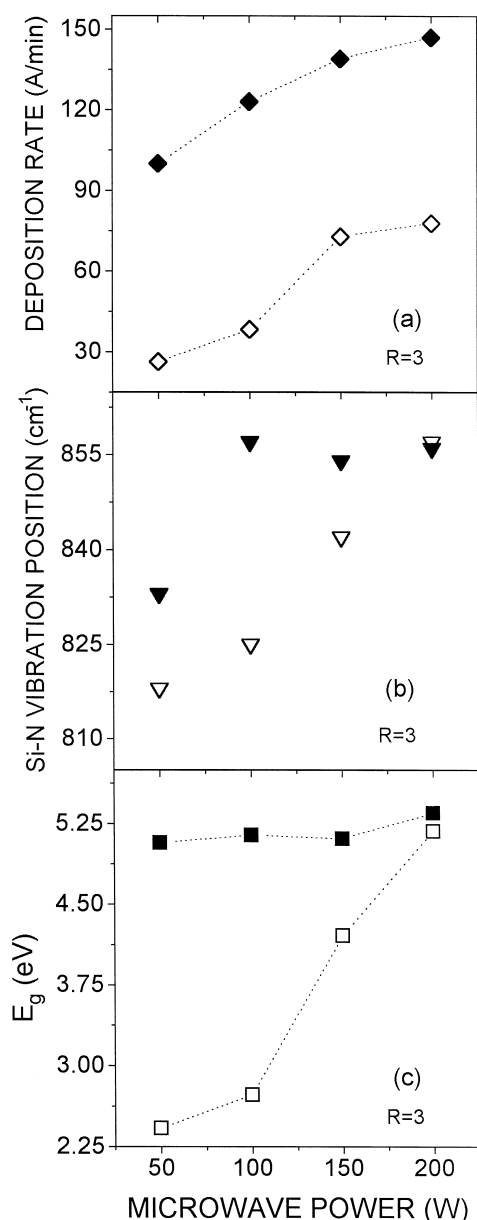


Fig. 2.

Fig. 2c displays the  $E_g$  values plotted versus the microwave power. The figure clearly shows the different role of the power in both reactors. The significant increase of  $E_g$  observed with the power in the Compact source would indicate a significative change of the film composition, from Si-rich to N-rich, as the highest  $E_g$  value is above 5.0 eV. On the contrary, in the AX4500 source, all values are almost similar ( $\sim 5.0$ – $5.2$  eV), which indicates that the microwave power has not influence on the film properties deposited using this source. The  $n$  results confirm this idea, as the values obtained for the films deposited using the AX4500 reactor are almost similar ( $\sim 1.90$ ), within the experimental error, when changing the microwave power in the 50–200 W range, while those obtained with the Compact source vary between 2.20 and 1.80 within the same power values.

### 3.3. Optical diagnosis of the discharge

Fig. 3 shows a typical  $N_2 + SiH_4$  spectrum of those obtained with both sources, in this case at 100 W and  $R = 3$ . The four main peaks observed in all spectra are those indicated in the figure for  $N_2^*$  and  $N_2^+$ . Those of the  $N_2^*$  molecule correspond to the vibrational absorption bands of the second positive system transition of  $N_2$  ( $C^3\Pi_u \rightarrow B^3\Pi_g$ ), at 315.9, 337.1, and 357.6 nm, corresponding to the (1,0), (0,0) and (0,1) transitions respectively. The peak located at 391.4 nm corresponds to the first negative system transition (0,0) of  $N_2^+$  ( $B^3\Sigma_u^+ \rightarrow X^2\Sigma_g^+$ ). In all cases, the absorptions related to neutral  $N_2^*$  have been stronger than those related to  $N_2^+$ , with intensities that depend on the power and on the plasma source used. Only one peak related to  $SiH_4$  has been observed at 288 nm,

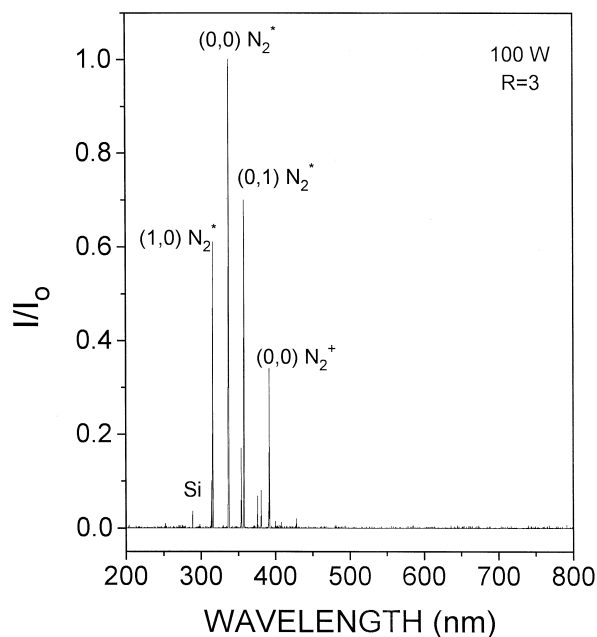


Fig. 3.

Table 2

Normalized intensities of the (1,0) and (0,1)  $N_2^*$  transitions, ( $I_1$  and  $I_2$ , respectively) and of the (0,0)  $N_2^+$  transition ( $I_3$ ) to the intensity of the (0,0)  $N_2^*$  transition ( $I_0$ ), in optical diagnosis spectra of discharges generated at different powers and  $R$  values using both sources

$R$	Power (W)	Compact-ECR			AX4500		
		$I_1/I_0$	$I_2/I_0$	$I_3/I_0$	$I_1/I_0$	$I_2/I_0$	$I_3/I_0$
1.6	100	0.50	0.69	0.44	0.64	0.82	0.26
3	100	0.61	0.75	0.35	0.69	0.73	0.26
3	50	0.56	0.80	0.62	0.69	0.66	0.49

As we explain in the text, the absolute value of  $I_0$  is higher in the AX4500 source than in the Compact one.

which corresponds to Si atoms, with low intensity in comparison to the stronger absorptions of  $N_2^*$ . The  $N_2^*$  peak located at 337.1 nm is found to be, in all cases, the strongest one in the spectra. In this way, all the other intensities have been normalized to the intensity of this peak for comparison between different spectra.

Table 2 presents the intensity of the (1,0) and (0,1)  $N_2^*$  transitions normalized to the (0,0)  $N_2^*$  intensity transition ( $I_1$ ,  $I_2$  and  $I_0$ , respectively), and the intensity of the (0,0)  $N_2^+$  transition ( $I_3$ ) also normalized to the  $I_0$  intensity for different powers and  $R$  in both reactors. It is worth nothing that the  $I_0$  line intensity is different from one source to the other, being higher in the AX4500. This mean that the absolute values of all the lines of the spectra are higher in the AX4500 source than in the Compact one. Comparing the results obtained at each deposition condition in both reactors, we observe there is no conclusion related to the  $N_2^*$  lines, but the trend which clearly appears is that the normalized  $I_3$  intensity increases as the microwave power decreases, similar for both sources.

## 4. Discussion

From the results about the film characterization presented in Section 3, it seems clear the different performances that both sources present with the deposition parameters. The differences should be attributed to the different discharge size, as no other design parameter has been changed. Published works on ECR discharges [7] assign the differences between discharges created with various reactors (electron temperature, plasma potential, ion energies) to the different discharge volume, which results in different diffusion length of the discharge,  $\Lambda$ , defined as:

$$\frac{1}{\Lambda^2} = \sqrt{\left(\frac{2.405}{r}\right)^2 + \left(\frac{\pi}{L}\right)^2}$$

where  $r$  and  $L$  are the inner radius and the height of the cylindrical quartz chamber, respectively. The parameter describe how varies the discharge size from a plasma source to another and can be roughly related with the mean

diffusion length of species within the plasma. The work of Sze and Asmussen [7], demonstrate that the coupling efficiency of the microwaves is optimum in discharges of moderate size for those is comprised between 1.5 and 2.5 cm.

The values of the diffusion length for the two sources here analyzed are  $\Lambda = 0.47$  cm. for the Compact source and  $\Lambda = 1.83$  cm. for the AX4500. From the analysis of the reactors and having in mind the work of Sze and Asmussen [7], we conclude several important questions in relation with the plasma properties of the two sources here used:

In the small source (Compact source), the diffusion length is well below the optimum value. As a consequence, high absorbed power densities, high wall erosion and high neutral and ion temperatures are expected. Indeed, a low microwave coupling efficiency is observed, with values for this parameter around 70% [7]. The films obtained with this source will suffer from contamination coming from wall erosion. This has been recently confirmed by us [16] and will be analyzed in the next paragraph. On the other hand, the ion and neutral bombardment of films during growth may severely affect the physical properties of  $\text{SiN}_x\text{:H}$  films. The results we have presented in the previous section seems to reinforce these conclusions. On the other hand, in the moderate size source (AX4500 source), the diffusion length is within the range of optimum values for this parameter. Then, the microwave coupling efficiency is high (typically, greater than 80% [7]) The plasma is now gentle, with high density and moderate ion and neutral energies. The films obtained with this reactor would exhibit good physical properties, like those showed in Fig. 1 and Fig. 2. Indeed, the wall erosion is low and films are obtained without contamination.

From the analysis of the results and from the previous discussion, we conclude that the higher coupling efficiency in the AX4500 reactor should result in more effectively excited and ionized species in the discharge, which produces high deposition rates (see Fig. 1a and Fig. 2a) and films with high N content in all cases, compared to those usually deposited by other plasma techniques. On the contrary, those films deposited with the Compact reactor, for which the coupling efficiency is lower, present properties that correspond to Si-rich compositions for a wide range of deposition parameters (low powers and  $R$  values), due to the low number of excited and ionized species in the discharge. Only for those films deposited at high nitrogen flows or high microwave powers, the reactions appear to be efficient enough to result in the deposition of near stoichiometric films (Fig. 2b and c) [11].

From the analysis of the optical diagnosis spectra of the plasma of both sources, we observe a different number of excited and ionized species present in the discharges, as all the peaks are always more intense in the plasma of the AX4500 source. These differences are not quoted in Table 2,

as the intensity of the  $I_0$  line are different from one source to the other and the values presented there are relative values and not absolute ones, as we have already explained in Section 3. From the data of Table 2 it is deduced that, in both reactors, when the absorbed power density is increased, the kinetic energy of electrons is also increased, so the dissociation of  $\text{N}_2$  is enhanced, resulting in both the decrease of  $\text{N}_2^+$  population and the increase of the excited species,  $\text{N}_2^*$ .

On the other hand, the deposition rate obtained with the Compact source is lower than that obtained with the AX4500 reactor in all cases (Fig. 2a). Regarding to the spectra obtained for each source at different microwave powers, also quoted in Table 2, we observe a similar relation between the relative population of ionized species,  $\text{N}_2^+$ , and the deposition rate: the normalized  $I_3$  intensity increases at the same time that the deposition rate decreases (i.e., decreasing microwave powers). Hence, it should be derived that the relative presence of  $\text{N}_2^+$  ions in the discharge results in a less effective film formation. The important conclusion derived from the optical diagnosis measurements is that the relative presence of  $\text{N}_2^+$  does not govern the formation of  $\text{SiN}_x\text{:H}$  films in ECR discharges, as some earliest works on this deposition methods state [17]. In fact, the results here presented together with previous studies [6,11], demonstrate that the deposition rate and the  $[\text{N}]/[\text{Si}]$  ratio in the films decreases as the  $I_3$  intensity increases.

Finally, we would like to make some comments in relation with the erosion of the chamber walls promoted by energetic ions in ECR discharges. We have previously demonstrated that the ions created in the discharge of the Compact source, under some deposition conditions (150–200 W and  $R > 5$ ), produce sputtering of the quartz liner located inside the plasma source, resulting in the incorporation of oxygen atoms into the  $\text{SiN}_x\text{:H}$  films (7 at.% about) [16]. On the contrary, the films deposited using the AX4500 reactor in the conditions more suitable for the sputtering with the Compact source (200 W and  $R = 9$ ) have reduced the oxygen content to 2 at.%, and below the detection limit for all other conditions. That confirms the higher ion energy and the higher power density in small sources, resulting in the larger heating of the walls predicted for this type of sources, which would result undesirable unless small size is necessarily required for applications such as in MBE machines.

## 5. Conclusions

Deposition rate, optical and bonding properties of  $\text{SiN}_x\text{:H}$  films deposited using two different sizes ECR source, and optical diagnosis spectra of the discharges have been analyzed. The films deposited using the smaller source, the Compact source, present characteristics which correspond to compositions between Si-rich and N-rich, as

the Si–H bond density (between  $0.5$  and  $2.5 \times 10^{22} \text{ cm}^{-3}$ ), the Si–N peak position ( $818$ – $840 \text{ cm}^{-1}$ ),  $E_g$  (between  $2.23$  and  $4.81 \text{ eV}$ ), and  $n$  (from  $2.27$  to  $1.80$ ) demonstrate. Those deposited with the moderate size AX4500 reactor present properties corresponding to stoichiometric and N-rich films, with Si–H bond density that is hardly measured, Si–N peak position between  $840 \text{ cm}^{-1}$  and  $870 \text{ cm}^{-1}$ ,  $E_g$  values that range from  $4.81 \text{ eV}$  to  $5.30 \text{ eV}$ , and  $n$  between  $2.15$  and  $1.90$ . Moreover, the deposition rate is more than three times higher in the AX4500 reactor with respect to the Compact source. The different performances of the sources have been attributed to the different diffusion length of the discharge, which in the case of the AX4500 source has the optimum value for the coupling efficiency of the microwave power into the discharge. A more intense  $\text{N}_2^+$  signal in the optical diagnosis spectra of the discharges taken at  $50 \text{ W}$  than those taken at  $100 \text{ W}$  has been observed, which is accompanied with a lower deposition rate and a more Si-rich character of the films. Therefore, it has been concluded that the presence of  $\text{N}_2^+$  in the discharge precludes the effective formation of the  $\text{SiN}_x\text{:H}$  films.

### Acknowledgements

The authors wish to thank Dr. E. Iborra at the E.T.S.I.T. of the Universidad Politécnica of Madrid for facilities offered in infrared measurements. This work has been

partly supported by the Spanish Government (CICYT) through grant No. TIC 93/0175.

### References

- [1] J. Pearton, C.R. Abernathy, F. Ren, *Appl. Phys. Lett.* 64 (1994) 2294.
- [2] W.H. Juan, S.W. Pang, *J. Vac. Sci. Technol. B* 12 (1994) 422.
- [3] S.V. Nguyen, K. Albaugh, *J. Electrochem. Soc.* 136 (1989) 2835.
- [4] J.C. Barbour, H.J. Stein, O.A. Popov, M. Yoder, C.A. Outten, *J. Vac. Sci. Technol. A* 9 (1991) 480.
- [5] J.R. Flemish, R.L. Pfeffer, *J. Appl. Phys.* 74 (1993) 3277.
- [6] S. Garcia, J.M. Martin, M. Fernandez, I. Martil, G. Gonzalez Diaz, *Phil. Mag. B* 73 (1996) 487.
- [7] F.C. Sze, J. Asmussen, *J. Vac. Sci. Technol. A* 11 (1993) 1289, and references therein.
- [8] W.A. Lanford, M.J. Rand, *J. Appl. Phys.* 49 (1978) 2473.
- [9] J.L. Hernandez-Rojas, M.L. Lucia, I. Martil, G. Gonzalez Diaz, J. Santamaria, F. Sanchez Quesada, *Appl. Optics* 31 (1992) 1606.
- [10] S. Garcia, J.M. Martin, I. Martil, G. Gonzalez Diaz, *Vacuum* 45 (1994) 1027.
- [11] S. Garcia, J.M. Martin, M. Fernandez, E. Iborra, I. Martil, G. Gonzalez Diaz, *J. Non-Cryst. Solids* 187 (1995) 329.
- [12] J. Robertson, *Phil. Mag. B* 69 (1994) 307.
- [13] W.R. Knolle, J. Osenbach, *J. Appl. Phys.* 58 (1985) 1248.
- [14] D.V. Tsu, G. Licovsky, *J. Vac. Sci. Technol. A* 4 (1986) 480.
- [15] S. Hasegawa, M. Matuura, H. Anbutu, Y. Kurata, *Phil. Mag. B* 56 (1987) 633.
- [16] S. Garcia, J.M. Martin, M. Fernandez, I. Martil, G. Gonzalez Diaz, *J. Vac. Sci. Technol. A* 13 (1995) 826.
- [17] T. Hirao, K. Setsune, M. Kitagawa, Y. Manabe, K. Wasa, S. Kohiki, *Jpn. J. Appl. Phys.* 26 (1987) L544.